Research Article
Cirrhosis

JOURNAL
OF HEPATOLOGY

Longitudinal neurometabolic changes in the hippocampus of a rat model of chronic hepatic encephalopathy

Graphical abstract

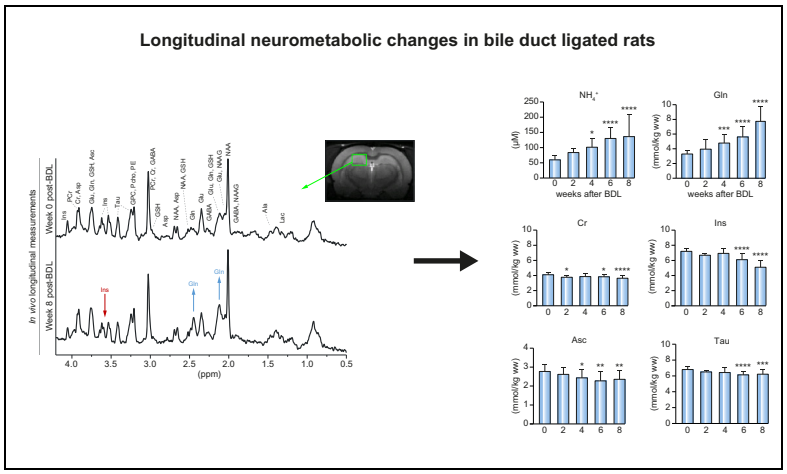

Highlights

- In hepatic encephalopathy, early neurometabolic changes occur 2–4 weeks post-bile-duct ligation.
- In hepatic encephalopathy, brain glutamine increases, but creatine and ascorbate decrease.
- Changes in astrocyte morphology are observed 4 weeks after bile-duct ligation.
- Early changes in hepatic encephalopathy are suggestive of osmotic/oxidative stress.
- Early changes in hepatic encephalopathy are accentuated 6–8 weeks after bile-duct ligation.

Authors

Olivier Braissant, Veronika Rackayová, Katarzyna Pierzchala, . . ., Jocelyn Grosse, Valérie A. McLin, Cristina Cudalbu

Correspondence

cristina.cudalbu@epfl.ch
(C. Cudalbu)

Lay summary

The sequence of events in chronic hepatic encephalopathy (HE) remains unclear, therefore using the advantages of *in vivo* proton magnetic resonance spectroscopy at 9.4T we aimed to test the hypothesis that neurometabolic changes are detectable very early in an established model of type C HE, offering insight into the primary events underpinning HE, before advanced liver disease confounds the findings. These early, previously unreported neurometabolic changes occurred as early as 2 to 4 weeks after bile-duct ligation, namely an increase in plasma ammonium and brain glutamine, a decrease in brain creatine and ascorbate together with behavioural and astrocyte morphology changes, and continued to progress throughout the 8-week course of the disease.

http://dx.doi.org/10.1016/j.jhep.2019.05.022
 J. Hepatol. 2019, 71, 505–515

Research Article
Cirrhosis

JOURNAL OF HEPATOLOGY

Longitudinal neurometabolic changes in the hippocampus of a rat model of chronic hepatic encephalopathy

Olivier Braissant[1,†], Veronika Rackayová[2,3,†], Katarzyna Pierzchala[3], Jocelyn Grosse[4], Valérie A. McLin[5], Cristina Cudalbu[3,*]

[1]*Service of Clinical Chemistry, University of Lausanne and University Hospital of Lausanne, Lausanne, Switzerland;* [2]*Laboratory of Functional and Metabolic Imaging, Center for Biomedical Imaging, Ecole Polytechnique Fédérale de Lausanne (EPFL), Lausanne, Switzerland;* [3]*Centre d'Imagerie Biomedicale (CIBM), Ecole Polytechnique Fédérale de Lausanne (EPFL), Lausanne, Switzerland;* [4]*Laboratory of Behavioral Genetics, Brain Mind Institute, School Of Life Sciences, Ecole Polytechnique Fédérale de Lausanne (EPFL), Lausanne, Switzerland;* [5]*Swiss Pediatric Liver Center, Department of Pediatrics, Gynecology and Obstetrics, University Hospitals Geneva, and University of Geneva Medical School, Switzerland*

Background & Aims: The sequence of events in hepatic encephalopathy (HE) remains unclear. Using the advantages of *in vivo* 1H-MRS (9.4T) we aimed to analyse the time-course of disease in an established model of type C HE by analysing the longitudinal changes in a large number of brain metabolites together with biochemical, histological and behavioural assessment. We hypothesized that neurometabolic changes are detectable very early, and that these early changes will offer insight into the primary events underpinning HE.

Methods: Wistar rats underwent bile-duct ligation (BDL) and were studied before BDL and at post-operative weeks 2, 4, 6 and 8 (n = 26). *In vivo* short echo-time ^{1}H-MRS (9.4T) of the hippocampus was performed in a longitudinal manner, as were biochemical (plasma), histological and behavioural tests.

Results: Plasma ammonium increased early after BDL and remained high during the study. Brain glutamine increased (+47%) as early as 2–4 weeks post-BDL while creatine (−8%) and ascorbate (−12%) decreased. Brain glutamine and ascorbate correlated closely with rising plasma ammonium, while brain creatine correlated with brain glutamine. The increases in brain glutamine and plasma ammonium were correlated, while plasma ammonium correlated negatively with distance moved. Changes in astrocyte morphology were observed at 4 weeks. These early changes were further accentuated at 6–8 weeks post-BDL, concurrently with the known decreases in brain organic osmolytes.

Conclusion: Using a multimodal, *in vivo* and longitudinal approach we have shown that neurometabolic changes are already noticeable 2 weeks after BDL. These early changes are suggestive of osmotic/oxidative stress and are likely the premise of some later changes. Early decreases in cerebral creatine and ascorbate are novel findings offering new avenues to explore neuroprotective strategies for HE treatment.

Lay summary: The sequence of events in chronic hepatic encephalopathy (HE) remains unclear, therefore using the advantages of *in vivo* proton magnetic resonance spectroscopy at 9.4T we aimed to test the hypothesis that neurometabolic changes are detectable very early in an established model of type C HE, offering insight into the primary events underpinning HE, before advanced liver disease confounds the findings. These early, previously unreported neurometabolic changes occurred as early as 2 to 4 weeks after bile-duct ligation, namely an increase in plasma ammonium and brain glutamine, a decrease in brain creatine and ascorbate together with behavioural and astrocyte morphology changes, and continued to progress throughout the 8-week course of the disease.

Introduction

Chronic hepatic encephalopathy (HE) is a complication of chronic liver disease (CLD) and is characterized by cognitive and motor deficits.[1–3] While minimal and overt HE may affect 20–70% of patients with CLD, the diagnosis is difficult in its early stages.[4,5] Tools enabling the detection of early neurometabolic changes in patients may allow for timely intervention, thereby minimizing the number of overt HE episodes and ensuing complications and costs.

Neurological alterations in HE are accepted to be the result of declining liver function, leading to impaired detoxification of ammonium (NH_4^+) and other substances that reach the brain.[3,6–11] Although the molecular mechanisms leading to HE remain unclear, NH_4^+ and glutamine (Gln) are a common thread in the complex and multifactorial model of HE pathogenesis. They are accepted to contribute to the incompletely understood metabolic cascades underlying the neurological manifestations of HE.

Gln synthesis in the central nervous system (CNS) is largely confined to astrocytes (glutamine synthetase activity[12]). In liver dysfunction or portosystemic shunting, increased NH_4^+ delivery to the brain increases astrocytic Gln, raising intracellular osmotic pressure and leading to astrocyte swelling and cytotoxic brain oedema.[13–16] In addition, increased astrocytic Gln can lead to the opening of the mitochondrial permeability transition pore

Keywords: In vivo proton magnetic resonance spectroscopy; Hepatic encephalopathy; Brain metabolism; Bile duct ligated; Rats; Chronic liver disease; Cholestasis.
Received 26 September 2018; received in revised form 24 May 2019; accepted 27 May 2019; available online 5 June 2019

* Corresponding author. Address: Centre d'Imagerie Biomedicale (CIBM), Ecole Polytechnique Fédérale de Lausanne (EPFL), EPFL-CIBM, Office F3 628, Station 6, CH-1015 Lausanne, Switzerland. Tel.: +41 21 693 7685.
E-mail address: cristina.cudalbu@epfl.ch (C. Cudalbu).
† Equal contribution of OB and VR.

and interfere with glutamatergic neurotransmission.[17–19] The mechanisms of NH_4^+ neurotoxicity also implicate oxidative/nitrosative stress, mitochondrial dysfunction, cell-signalling disruption, neuroinflammation and alterations in neuronal process growth.[9,10,16,20–24] While all these mechanisms appear implicated in the pathogenesis of HE, the sequence of events remains unclear, owing largely to the lack of reliable longitudinal studies.

In vivo proton magnetic resonance spectroscopy (^{1}H-MRS) is widely used to investigate brain metabolism non-invasively, allowing for longitudinal follow-up of disease and response to treatment. ^{1}H-MRS was among the first techniques to provide indirect evidence *in vivo* of osmoregulatory disturbances: an increase in the sum Gln + glutamate (Glu; Gln + Glu = Glx) concentration together with a decrease in brain osmolyte myo-inositol (Ins).[16] These changes have since been thought to underlie the low grade cerebral oedema observed in chronic HE in humans. Later, other magnetic resonance imaging (MRI) techniques (*i.e.* diffusion weighted/tensor imaging, water mapping) further expanded our understanding of chronic HE by demonstrating the presence of low grade cerebral oedema.[13,25–28] Although these studies were instrumental in demonstrating neurometabolic disturbances, their contribution was limited by comparatively low magnetic field strengths used and the ensuing limitation in the number of metabolites quantified (*i.e.* Glx, total creatine (tCr), total choline (tCho) and Ins[5,28–31]). Therefore, present day availability of very high magnetic field strengths (≥7T) combined with spectra acquisition at very short echo times (<10 ms) offer unprecedented opportunities to further understand the longitudinal neurometabolic events of chronic HE in detail by expanding the number of brain metabolites detectable *in vivo* to about 18 both in animal models and humans.[32–35]

The bile-duct ligation (BDL) rat model is accepted by ISHEN (International Society for Hepatic Encephalopathy and Nitrogen Metabolism) as a model of type C HE, namely HE associated with liver disease, portal hypertension and hyperammonemia.[36] To date, the few studies in this model have used *in vivo* or *ex vivo* ^{1}H-MRS combined with MRI or behavioural tests at late time points. The main findings of these studies were that plasma NH_4^+ and brain Gln increased while other brain osmolytes decreased (Ins and tCho). They also brought controversial data regarding fluctuations in lactate (Lac), Glu, N-acetyl-aspartate (NAA) and brain water content.[26,37–39] Further studies are required to understand the significance of these findings and to comprehend the chronology of events leading to these metabolic perturbations, including early molecular and cellular brain changes which may offer insight into the primary mechanisms of HE.

Thus, we aimed to use a multimodal and longitudinal approach to test the hypothesis that neurometabolic changes are detectable very early on in the course of CLD. Using the advantages of high field spectroscopy, we would therefore be able to analyse the longitudinal changes in tissue osmoregulation, neurotransmission, oxidative stress and energy metabolism leading to the well-characterized end-stage events in the BDL rat model, bringing important insight into the chronology of events leading to HE. We combined *in vivo* longitudinal ^{1}H-MRS at very high magnetic field (9.4T) and short echo time (TE = 2.8 ms) in the hippocampus, with biochemical, histological analysis and behavioural studies. The rationale was to identify an unprecedented number of brain metabolites involved in chronic HE at key time points and analyse their implications at the molecular and tissue levels during the course of chronic HE in an established animal model.

Materials and methods

BDL rat model for CLD

All experiments were approved by the Committee on Animal Experimentation for the Canton de Vaud, Switzerland (VD3022/VD2439). Wistar male adult rats (n = 44, 150–175 g, Charles River Laboratories, L'Arbresle, France) were used: 26 rats underwent BDL while 18 rats were sham-operated. Experiments were performed before BDL (week 0) and at post-operative weeks 2, 4, 6 and 8 using isoflurane anaesthesia. Early changes were defined as changes happening between weeks 0–4, and late changes those happening beyond week 4. The 4-week limit was based on 2 factors: i) animal half-life in this model and ii) time until animals showed minimal signs of disease and steady weight gain.

Validation of the CLD-induced HE in BDL rats: biochemical and behavioural measurements

The following liver parameters were quantified on Integra© or COBAS8000© analysers (Roche, Switzerland): plasma NH_4^+ (n = 17), total bilirubin (n = 18), alanine aminotransferase (ALT; n = 14) and gamma-glutamyltransferase (GGT; n = 12).

To test the presence of fine motor deficits (characteristic of chronic HE), locomotor activity was assessed in the open field test. The following parameters were evaluated using video tracking system (Noldus Ethovision software 11.5): frequency of crosses, percent time spent, latency to enter each zone [s], distance moved [m] and velocity [cm/s]. These parameters were calculated for the entire 10 min of the open field test. A total of 17 BDL and 7 sham-operated rats were observed at 4, 6 and 8 weeks post-operation.

In vivo ^{1}H-MRS

In vivo ^{1}H-MRS measurements were performed longitudinally on a horizontal actively shielded 9.4T magnet using the SPECIAL sequence (TE = 2.8 ms) in a volume of interest (VOI) of $2 \times 2.8 \times 2$ mm^3 positioned in hippocampus, a key region implicated in cognitive deficits (*i.e.* learning, memory) observed in chronic HE.[3] A total of 18 brain metabolites were quantified using LCModel and water as internal reference. ^{1}H-MRS was performed before BDL (week 0; n = 26) and at post-operative weeks 2 (n = 10), 4 (n = 26), 6 (n = 22) and 8 (n = 22). Each animal served as its own control, compared to week 0. Animals were sacrificed at post-operative weeks 4 (n = 4 for BDL rats and n = 4 for sham-operated rats) and 8 (n = 7 for BDL rats and n = 7 for sham-operated rats), after ^{1}H-MRS, for histological measurements.

Immunohistochemistry

A mouse monoclonal anti-glial fibrillary acidic protein (GFAP; MAB360 Merck Millipore) antibody was used to characterize astrocyte morphology and counterstained with DAPI (nucleus labelling, blue fluorescence, D1306, Thermofisher). To monitor the suspected change in water and ion balance in the brain tissue of BDL rats, a rabbit polyclonal anti-aquaporin 4 (AQP4; AB3594 Merck Millipore) antibody was used. Secondary antibodies were goat or rat anti-mouse or anti-rabbit IgG labelled with Alexa Fluor® 488 (green; Thermo Fisher Scientific), Alexa Fluor® 555 (red; Life Technologies) or Alexa Fluor® 594 (red; Jackson ImmunoResearch Europe Ltd). Sholl analysis of astrocytes is described in detail in the Supplementary information.

Statistical analysis

Results are presented as mean ± SD and % increase/decrease compared to week 0. One-way ANOVA (Prism 5.03, Graphpad, La Jolla CA USA) with respect to each metabolite in the neurochemical profile followed by Bonferroni's multi-comparisons post-test (weeks post-BDL, total of 10 comparisons) were used. For behavioural tests and Sholl analysis of astrocytes, 2-way ANOVA followed by Bonferroni's multi-comparisons post-test were used to compare BDL and sham-operated rats. All tests were 2-tailed. Pearson correlation analysis was performed on all longitudinally acquired data to test for correlations between brain metabolites, plasma values and behavioural tests. Of note, correlations between brain metabolites and behavioural tests were not performed since the hippocampus is known for its role in cognition/memory rather than motor coordination. Significance in all tests was attributed as follows: $^{*}p$ <0.05; $^{**}p$ <0.01; $^{***}p$ <0.001; $^{****}p$ <0.0001.

For further details regarding the materials used, please refer to the Supplementary information.

Results

Validation of the CLD-induced HE in BDL rats by biochemical and behavioural measurements

Plasma values were in normal ranges for all rats before BDL, while NH_4^+ and bilirubin (Fig. 1A) rose following BDL. The Fig. S1 shows the weight of the BDL animals. BDL rats travelled a shorter distance than sham-operated animals at week 4 post-BDL (−24%), and this distance continued to decrease, reaching −54% at week 8 (Fig. 1B). There was no difference between BDL and sham rats for the following: time spent in the wall-zone, centre-zone and inter-zone, and latency to enter centre-zone (Fig. S2), suggesting animal anxiety was not a variable.

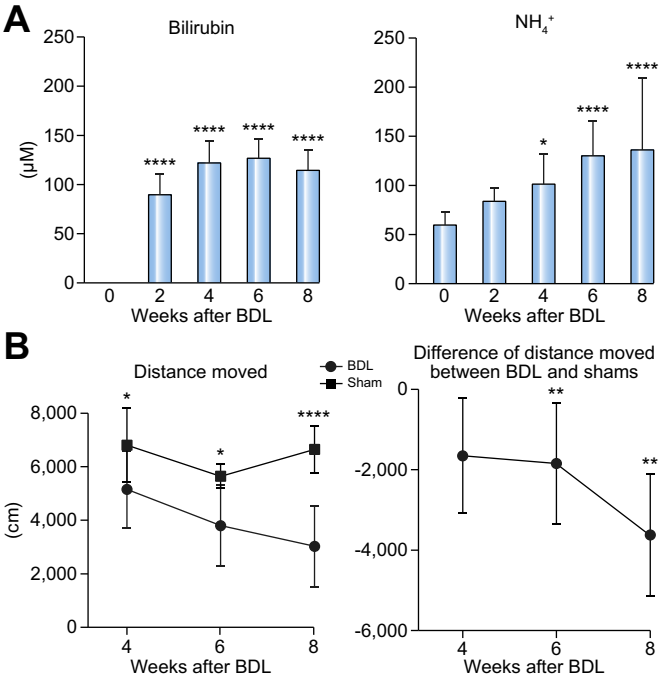

Fig. 1. BDL-induced changes in plasma total bilirubin, NH_4^+ and distanced travelled. (A) Longitudinal changes of plasma total bilirubin and NH_4^+. Bilirubin was non-measurable before BDL. (B) Distance travelled by BDL and sham-operated rats. Mean ± SD. Significance level between weeks 0 and 2–8: $^{*}p$ <0.05, $^{**}p$ <0.01, $^{***}p$ <0.001, $^{****}p$ <0.0001 (1-way [plasma] and 2-way [distance] ANOVA). BDL, bile-duct ligation.

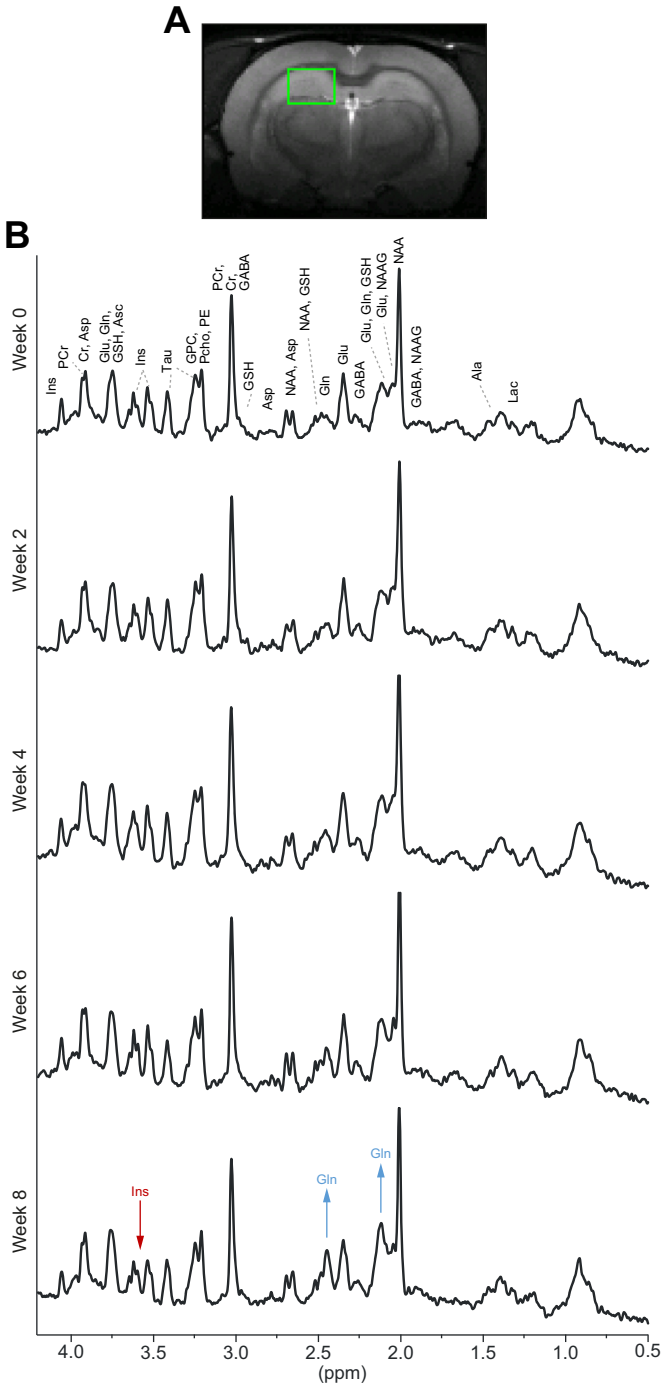

Fig. 2. Representative *in vivo* ^{1}H-MRS spectra acquired longitudinally in 1 BDL rat at 9.4T: (A) Anatomical T_2 weighted image showing the hippocampus ^{1}H-MRS voxel (green). (B) Brain ^{1}H-MRS spectra measured before BDL and at post-operative weeks 2–8; Gln increase and Ins decrease is clearly visible. ^{1}H-MRS, proton magnetic resonance spectroscopy; Ala, alanine; Asc, ascorbate; Asp, aspartate; BDL, bile-duct ligation; Cr, creatine; GABA, γ aminobutyric acid; Glc, glucose; Gln, glutamine; Glu, glutamate; GPC, glycerophosphocholine; GSH, glutathione; Ins, myo inositol; Lac, lactate; NAA, N acetylaspartate; NAAG, N acetylaspartylglutamate; PCho, phosphocholine; PCr, phosphocreatine; PE, phosphoethanolamine; Tau, taurine. (This figure appears in colour on the web.)

BDL-induced increase in cerebral Gln and decrease in other osmolytes, antioxidants and neurotransmitters, measured by ^{1}H-MRS

The first metabolite to increase was Gln at week 2 (compared to week 0), reaching significance at week 4 (+47%) and showing a gradual increase towards +136% at week 8 (Figs. 2, 3, Table S1). The NH_4^+-induced increase in Gln was followed by a decrease in several metabolites commonly accepted as CNS osmolytes and brain cell volume regulators (Ins, tCho, taurine (Tau), creatine (Cr), phosphocreatine (PCr))[40–42] (Figs. 2, 3, Table S1). Ins showed a significant decrease at week 6 (−15%) and reached −30% at week 8. Similarly, tCho (glycerophosphocholine (GPC) + phosphocholine (PCho)) showed a progressive decline reaching a significant −26% decrease at week 8 (Figs. 2, 3, Table S1). Tau showed a −9% decrease from week 0 to week 8 (Figs. 2, 3, Table S1). Cr displayed an early and statistically significant decrease at week 2, reaching a −11% decrease from week 0 to week 8 (Figs. 2, 3, Table S1).

Next, we computed the sum of the main cerebral organic osmolytes to evaluate the osmoregulatory response to the Gln-induced osmolar stress (Fig. 4). The sum which included Gln appeared to be constant (Fig. 4B), while the same sum without Gln showed a rapid decrease as early as 2 weeks post-BDL, reaching statistical significance at 6 weeks and −16% at 8 weeks post-BDL (Fig. 4C). However, the absolute increase in Gln was slightly higher than the decrease in other organic osmolytes (at 8 weeks post-BDL: Gln: +4.4 mmol/kg_{ww} *vs* sum of osmolytes: −3.8 mmol/kg_{ww}, Fig. 4D).

Among neurotransmitters, only Glu showed a late significant decrease at week 6, reaching −11% at week 8, while aspartate (Asp) and γ-aminobutyric acid (GABA) showed no significant changes (Fig. 3). In addition, NAA, a neuronal marker,[43] did not display any changes during the course of the study. Lac, a metabolite involved in CNS energy metabolism, showed a tendency to increase at week 8, although this finding did not reach statistical significance (+10%). PCr displayed no changes throughout the course of the study even though Cr showed a significant decrease (Fig. 3). This decrease in Cr was associated with a significant decrease of tCr (−8%).

Finally, looking at antioxidants, ascorbate (Asc) showed an early and statistically significant decrease at week 4 compared to week 0 (−12%) and reached −15% at week 8, while no

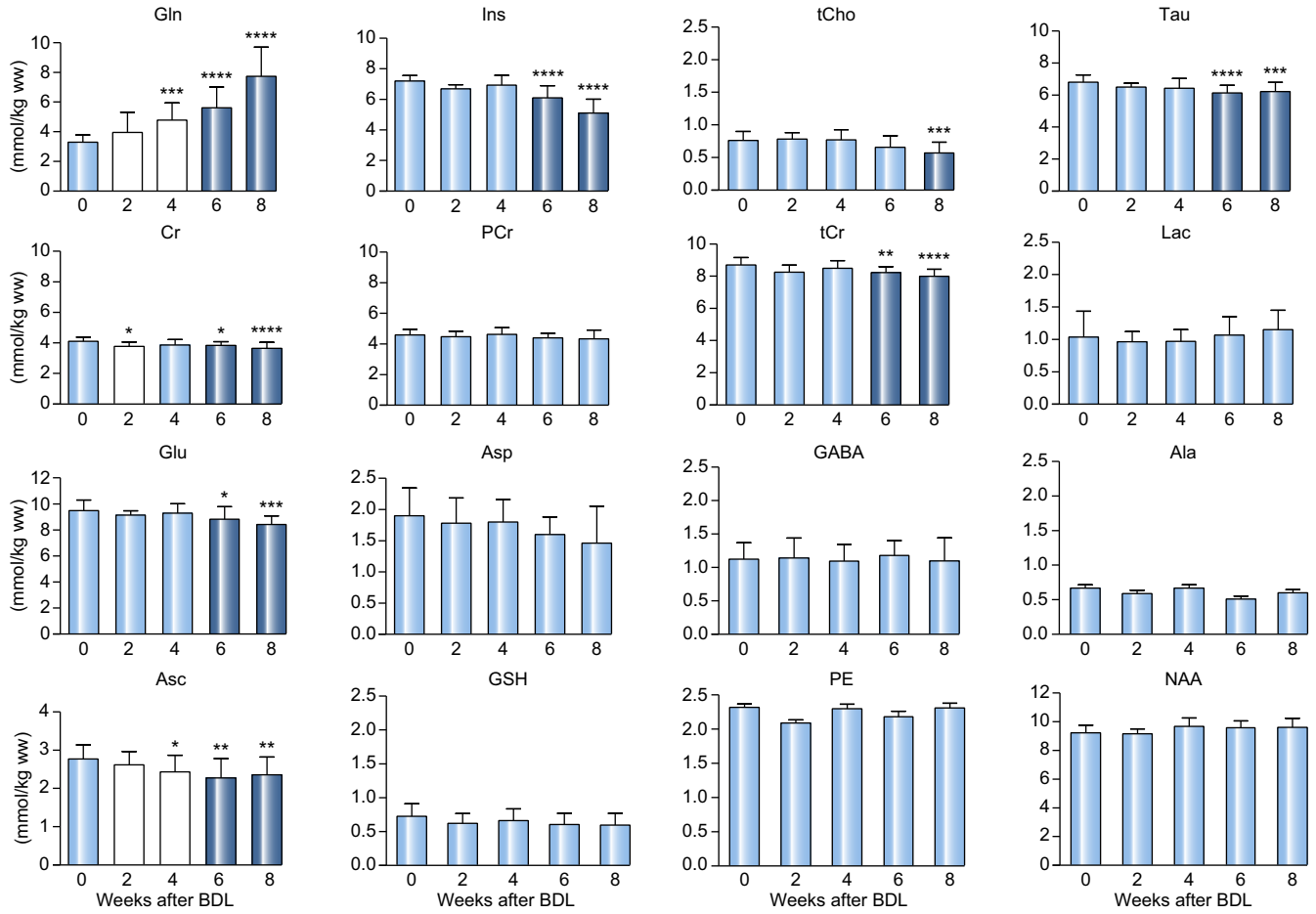

Fig. 3. Longitudinal ^{1}H-MRS data of the main brain metabolites from 0 to 8 weeks post-BDL. Mean ± SD, significance level between weeks 0 and 2–8: *p <0.05, **p <0.01, ***p <0.001, ****p <0.0001 (1-way ANOVA), metabolite concentrations at week 0 and those of metabolites showing non-significant changes are shown in light blue, while the early changes are shown in white and late changes in dark blue. ^{1}H-MRS, proton magnetic resonance spectroscopy; Ala, alanine; Asc, ascorbate; Asp, aspartate; BDL, bile-duct ligation; Cr, creatine; GABA, γ aminobutyric acid; Glc, glucose; Gln, glutamine; Glu, glutamate; GPC, glycerophosphocholine; GSH, glutathione; Ins, myo inositol; Lac, lactate; NAA, N acetylaspartate; NAAG, N acetylaspartylglutamate; PCho, phosphocholine; PCr, phosphocreatine; PE, phosphoethanolamine; Tau, taurine; tCho, total choline (GPC + PCho); tCr, total creatine (Cr + PCr).

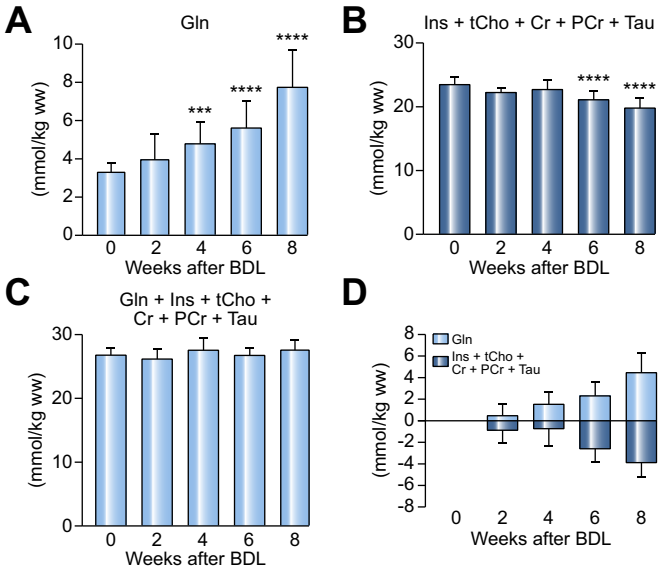

Fig. 4. Sum of main brain organic osmolytes in BDL rats. (A) Longitudinal increase in brain Gln. (B) Longitudinal evolution of the sum of different brain organic osmolytes including Gln and (C) without Gln. (D) Absolute increase in Gln compared to the decrease in the main organic osmolytes. Mean ± SD, significance level between weeks 0 and 2–8: ***p <0.001, ****p <0.0001 (1-way ANOVA). BDL, bile-duct ligation; Cr, creatine; Gln, glutamine; GPC, glycerophosphocholine; Ins, myo inositol; PCho, phosphocholine; PCr, phosphocreatine; Tau, taurine; tCho, total choline (GPC + PCho); tCr, total creatine (Cr + PCr).

significant changes were observed for glutathione (GSH), even though a slight decrease was noticed over the course of the study (Fig. 3).

Astrocyte changes and dysregulation of AQP4 in BDL rats

Using GFAP staining, we demonstrated that BDL rats, compared to sham-operated controls, developed time-dependent changes in astrocyte morphology, observable starting at 4 weeks post-BDL and increasing until 8 weeks post-BDL (Fig. 5A,B). Astrocytes showed a thickening of their main proximal processes, as well as retraction (shortening of processes length measured on sections: week 4 post-BDL: −13%, p <0.0001; week 8 post-BDL: −32%, p <0.0001). They also displayed a decrease in number of processes (decreased number of intersections, depending on the distance from the cell body: week 4 post-BDL: up to −45%, p <0.005; week 8 post-BDL: up to −73%, p <0.0001) (Fig. 5A). In parallel, AQP4 staining, expressed in astrocytic feet lining microcapillaries, as well as within microcapillary endothelial cells at blood brain barrier (BBB), was increased in the hippocampus of BDL rats (weeks 4 and 8 post-BDL) as compared to sham-operated animals (Fig. 5C,D).

Pearson correlations between brain metabolites, plasma values and behavioural tests

Pearson correlation coefficients were used to identify dependences between measured parameters with the goal of highlighting metabolic pathways involved in the neurological changes associated with type C HE (Fig. 6). First, the correlation between brain Gln and plasma NH_4^+ was highly significant (r = 0.61, p ≤0.0001). As these 2 metabolites are considered responsible for many of the changes in HE, we further evaluated the correlations between plasma NH_4^+ or brain Gln with other metabolites or study parameters. Elevation of plasma NH_4^+ correlated with the decrease in distance moved (r = −0.60, p ≤0.0001). The correlation between brain Cr and brain Gln

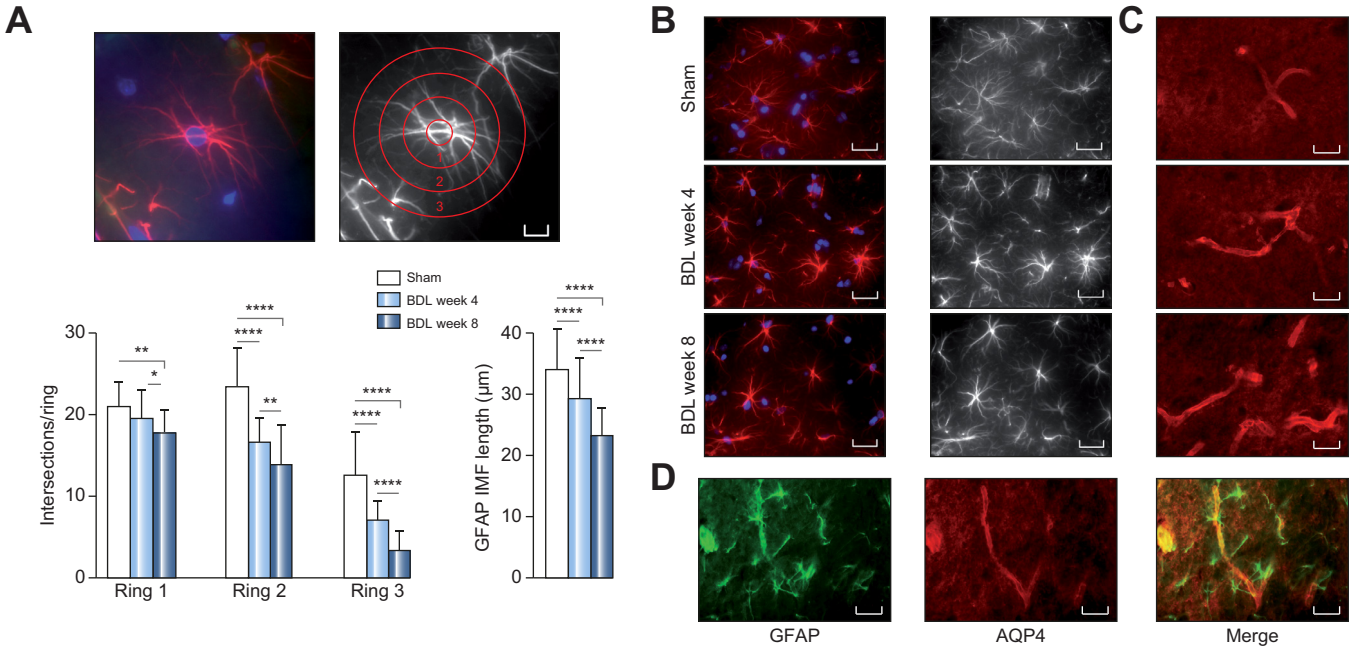

Fig. 5. Astrocytic dysregulation in hippocampus (hilus) of BDL rats: (A-B) GFAP with nuclei DAPI co-labelling (blue) and (C-D) AQP4 and co-expression of GFAP (green) and AQP4 (red) in astrocytes and on microcapillary endothelial cells at BBB in BDL compared to sham-operated rats, at 4 and 8 weeks post-BDL. Scholl analysis of GFAP-labelled astrocytic processes showed a significant time-dependent decrease of both the number (measured as decrease in intersections in each of the 3 concentric rings) and the mean length of processes observable within the section (A). BDL led to increased AQP4 expression in both the astrocytic feet lining microcapillaries and microcapillary endothelial cells at BBB (C-D). Representative pictures taken from BDL and sham rats. Bar: 10 µm (A) and 25 µm (B-D). Details of Sholl analysis are in the supplementary information; *p <0.05, **p <0.01, ****p <0.0001; Mean ± SD. AQP4, aquaporin-4, BBB, blood brain barrier; BDL, bile-duct ligation; GFAP, glial fibrillary acidic protein.

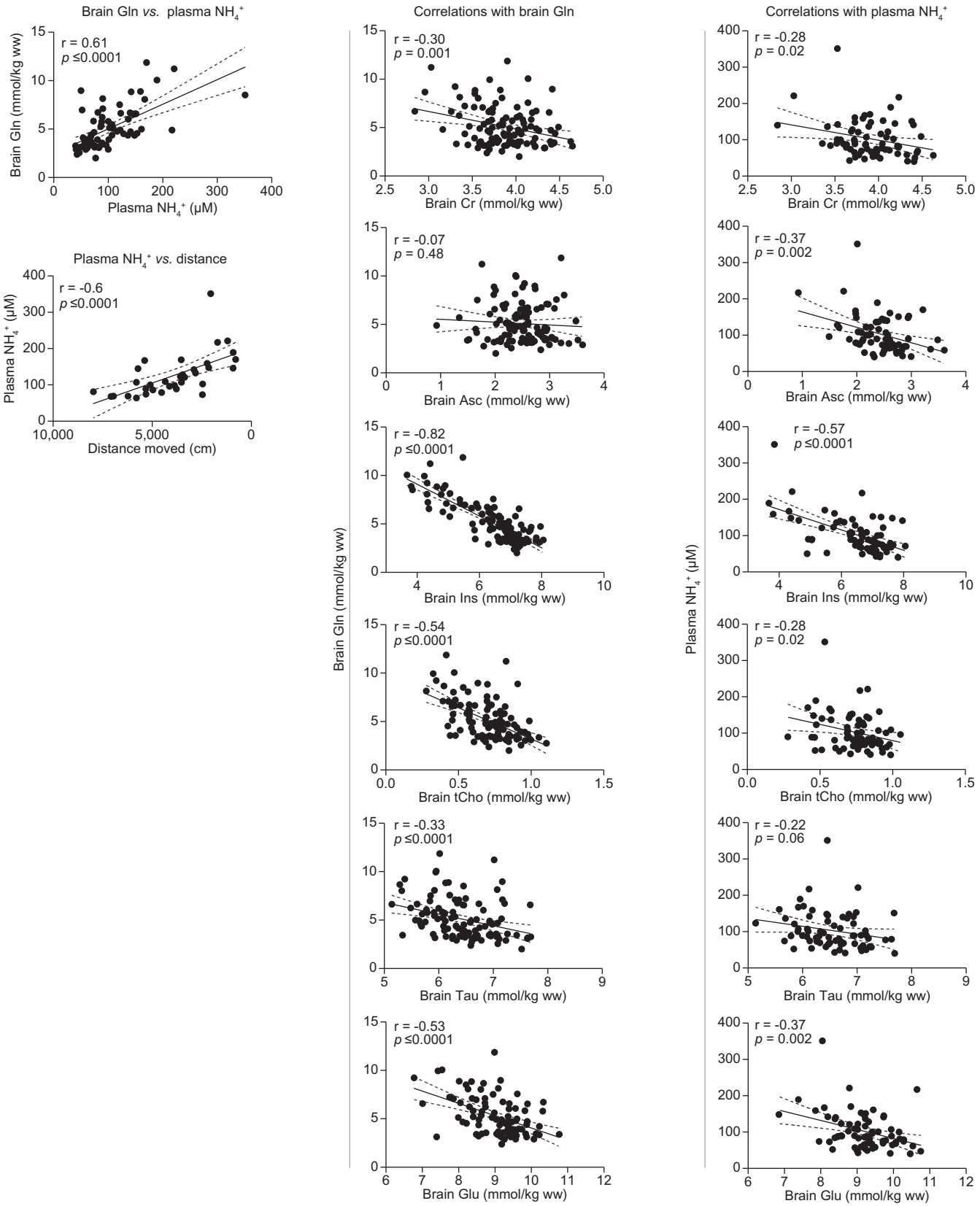

Fig. 6. Pearson correlations between plasma NH_4^+, brain metabolites and distance moved over the duration of the entire study. Pearson correlation coefficients (r) and corresponding *p* values are shown together with 95% confidence bands (doted lines) surrounding the best-fit line (linear regression). All the longitudinally acquired data were used. Asc, ascorbate; Cr, creatine; Gln, glutamine; Glu, glutamate; GPC, glycerophosphocholine; Ins, myo inositol; PCho, phosphocholine; Tau, taurine; tCho, total choline (GPC + PCho).

was stronger ($p = 0.001$) than the one with plasma NH_4^+ ($p = 0.02$). In contrast, plasma NH_4^+ showed a significant correlation with brain Asc ($p = 0.002$), while brain Gln showed no correlation ($p = 0.48$). As expected, brain Gln showed stronger correlations with the other brain osmolytes (Ins, tCho, Tau) than plasma NH_4^+. In addition, Glu strongly correlated with brain Gln ($p \leq 0.0001$), while the correlation with plasma NH_4^+ was less pronounced ($p = 0.002$).

We also identified additional correlations between Glu and Cr, and Glu and other osmolytes (data not shown). These correlations are most likely the direct consequence of increased brain Gln. Given that their biological relevance is not yet understood, these correlations will not be discussed further.

Discussion

The present study shows for the first time that significant neurometabolic changes are present in the rat hippocampus as early as 2–4 weeks after BDL: increases in plasma NH_4^+ and brain Gln, decreases in brain Cr and Asc, decreases of distance moved, and dysregulation of astrocyte morphology. These compelling and novel findings are likely the premise of later changes and raise the question of whether similar changes might exist in humans but are missed owing to ^{1}H-MRS methodological limitations both in field strength and echo times.

Early neurometabolic events in CLD

Little is currently known about the early neurometabolic events associated with CLD, something which we aimed to analyse using a detailed, longitudinal, *in vivo* analysis of an established model of type C HE at 4 time points. We reasoned that focusing on early metabolic changes might shed light on which neurometabolic alterations are secondary to CLD alone, prior to the onset of complications associated with advanced, decompensated liver disease such as ascites, bleeding, infections, and malnutrition.[4] Indeed, as early as 2 weeks post-BDL we observed increased plasma NH_4^+ (and bilirubin), brain Gln and decreased brain Cr and Asc (Fig. 3). Given the ongoing progression of these early metabolic changes, they might be the biologically relevant premise underlying the histological and potentially the behavioural changes at 4 weeks and beyond (Figs. 3 and 6), together with other factors not assessed herein. Since BDL rats at early time points were otherwise well and displayed satisfactory weight gain, the behavioural modifications at 4 weeks post-BDL are most likely attributable to early HE rather than secondary to systemic repercussions of end-stage liver disease.

Brain Gln and plasma NH_4^+ were highly correlated in our BDL rats (Fig. 6), suggesting that Gln is probably the first metabolite influenced by increasing plasma NH_4^+, in agreement with our previous work.[38] In addition, changes in plasma NH_4^+ correlated with the decrease in distance moved over the 8-week course of the disease (Fig. 6). These findings have been historically difficult to verify in CLD for several reasons. First, plasma NH_4^+ levels in CLD are both lower and more variable than in acute liver failure.[8] Second, the use of low magnetic fields may have been limiting in human studies where brain Gln is not reliably quantified. Finally, very few studies have been performed in animal models to date. Only rare studies have identified a correlation between plasma NH_4^+ and brain Gln or severity of HE in CLD,[29,44–46] while others did not find any correlation.[37]

The behavioural changes observed in BDL rats are of interest since it is well known that patients with chronic HE exhibit impaired motor function,[3,47] something also observed previously in rats 6 weeks post-BDL together with a decreased discrimination index for short term memory,[48,49] altered spatial working and spatial reference memory (prefrontal cortex and hippocampal functions, respectively).[50] Although the molecular underpinnings are still elusive, a number of neurotransmitter systems have been proposed to be involved.[48,51]

NH_4^+-induced oxidative and nitrosative stress in CNS is believed to play a role in the pathogenesis of HE, and there is growing evidence that osmotic and oxidative stress are closely related.[52,53] Although Asc is an important CNS antioxidant preferentially located in neurons,[54] the present study is the first to report an *in vivo* measurable Asc decrease in a model of chronic HE, occurring as early as 4 weeks post-BDL. The decrease in Asc concentration over time correlated mainly with the rise in plasma NH_4^+ (Fig. 6). Given that there was no correlation observed with brain Gln, this finding suggests a direct effect of NH_4^+ on CNS antioxidant pathways.[52] The presence of systemic oxidative stress has also been shown in BDL rats. Likewise, the synergistic effects of both NH_4^+ and systemic oxidative stress have been shown to increase brain water content.[55] A close relationship was also previously shown between NH_4^+, precipitating factors, Gln, astrocyte swelling, NMDA receptor activation, oxidative stress, and the auto-amplificatory loop between astrocyte swelling and oxidative stress.[4,16,52] All these factors lead to altered astrocyte function, glial/neuronal communication and multiple neurotransmitter systems, and thus impact synaptic plasticity and cerebral networks which may account for the signs and symptoms of HE.[4,16,52]

It is commonly accepted in chronic HE that increased plasma NH_4^+ generates a rise in the osmolyte Gln leading to osmotic imbalance followed by a partial compensation through the gradual decrease of other brain osmolytes (Ins, tCho, Tau and Cr), thus leading to low grade brain oedema.[5,13–16,38,45] Previous studies in BDL rats have reported an increase in brain water content (from ~76% to ~78% at 4 weeks or from ~78% to ~79% at 6 weeks post-BDL), while no changes were reported by other studies.[39,55–57] The changes in brain water content appear to be small 1–2% and sometimes difficult to assess.[13,58] However, this does not exclude the presence of astrocytic osmotic stress and/or morphological changes.[59] Although several hypotheses have been elaborated to explain the relationship between neurometabolic changes, cell swelling/oedema and neurological outcome in chronic HE, these remain controversial.

Among the potential metabolites implicated in osmoregulation, Cr was the first to decrease, as early as 2 weeks post-BDL (Fig. 3). This decrease in hippocampal Cr correlated significantly with brain Gln rise. The correlation was less strong with plasma NH_4^+ (Fig. 6), suggesting that the Cr decrease is a direct compensatory mechanism to Gln osmotic stress. While Cr has been shown to efflux from astrocytes following osmotic challenge,[60,61] we cannot exclude neuronal efflux as a mechanism for this decrease in Cr. This is particularly relevant in the hippocampus given that hippocampal neurons are both known to harbour very high concentrations of Cr and to synthesize it.[42,62] The release of osmotically active Cr by neurons in response to increases in Gln may hamper their function under CLD conditions, as their rate of Cr utilization is known to be high.[63] The other measurable brain organic osmolytes (*i.e.* Ins,

Tau, tCho) showed only a trend toward a decrease during this early period.

Several changes were observed in astrocyte morphology starting 4 weeks post-BDL: decreased number and shortening of processes, as well as thickening of proximal processes. These findings were further corroborated by an increase of AQP4 (a plasma membrane protein regulating water transport and homeostasis[41]) expression on the astrocytic feet around BBB and in microcapillary endothelial cells forming the BBB, a finding previously reported in cultured astrocytes exposed to ammonia and in BDL rats.[64,65] Our data suggest that BDL-induced imbalance in osmolytes, as shown by ^{1}H-MRS together with increased AQP4 immunostaining, likely leads to early osmotic stress. The observed changes in astrocyte morphology might also be linked to their reactivity as previously shown in hyperammonemic rats without CLD,[66] findings which need further validation in BDL rats. Moreover, it has been previously shown that hyperammonemia and inflammation cooperate in inducing the neurological alterations in HE probably through altered neurotransmission.[21,51,67] Therefore, our findings add to the body of literature by suggesting that early neurometabolic changes reflecting osmotic/oxidative stress and the related changes in astrocyte morphology might underlie the early neurobehavioral manifestations of HE among other existing factors, such as neuroinflammation and neurotoxins all of which are linked in a self-amplifying loop.[4,11,21,23,52,66] Histological studies of BDL rat brains are controversial, some reporting no change, increased or decreased of GFAP staining in different brain regions.[26,68,69] Regarding AQP4, a recent study showed reduced expression in the olfactory bulb and prefrontal cortex in BDL rats.[50] Thus, additional studies in BDL rats would be useful to further our understanding of the changes/mechanisms/factors implicated in this animal model.

We observed a rapid decrease of the sum of osmolytes ($\sim$0.87 mmol/kg$_{ww}$) as early as 2 weeks post-BDL (Fig. 4C), concomitant to Gln increase. Despite this prompt osmoregulatory response to the early rise in plasma $NH_4^+$and brain Gln, astrocytes displayed signs of osmotic/oxidative stress at 4 weeks post-BDL as shown by ^{1}H-MRS, which coincided with the first observed astrocytic and behavioural changes, suggesting that osmoregulation was insufficient. Several reasons may explain the apparent discrepancy between the rapid and ongoing osmotic response in hippocampus of BDL rats and the astrocytic osmotic imbalance observed later on. First, osmolytes are measured as a mean in the voxel, which is not representative of cellular osmoregulation. Second, most of these metabolites are differentially distributed among CNS cell types and cellular compartments, making it difficult to decipher their respective roles in osmoregulation using MRS. For example, Ins is preferentially concentrated in astrocytes, Tau in neurons, while Cr is ubiquitous.[62,70,71] Third, choosing which metabolites to include in the sum is difficult for 2 reasons: the osmoregulatory role of some metabolites is controversial and osmotically active small ions (*e.g.* Na^+, K^+, Ca^{2+}, Cl^-) and proteins, which also play important roles in osmoregulation, are not measurable by ^{1}H-MRS. Finally, brain NH_4^+ also acts as an osmolyte before being converted to Gln which might explain its correlation with Ins. A previous study[37] which reported higher brain osmolytes (sum of Gln, Glu, Ins, Tau) in BDL rats compared to sham-operated rats concluded that brain osmoregulation cannot compensate for the increase in both brain Gln and Lac. In contrast to this study, we chose not to include Glu in our osmotic calculations, because most Glu is localized in synaptic vesicles and therefore does not contribute significantly to osmotic pressure in the cytoplasm.

Late neurometabolic events in CLD

Unlike previous studies, we followed rats to 8 weeks post-BDL. To the best of our knowledge, there is only 1 published study of brain metabolism in BDL rats using *in vivo* ^{1}H-MRS,[39] examining rats at 4, 5 and 6 weeks post-BDL using a larger voxel ($6.5 \times 6.5 \times 6.5$ mm^3). It showed increased brain Gln and decreased Ins and tCho, in agreement with our results, but is of limited use for comparison with our data given the limited temporal analysis.

As expected,[38] brain Gln and plasma NH_4^+ continued to increase beyond the 4th week after ligation reaching a more than 2-fold increase at 8 weeks (Figs. 1 and 3) in line with the stronger decrease of other major brain osmolytes. Ins showed the strongest relative and absolute decrease ($-$30%). It was followed by Tau, Cr and consequently tCr. tCho showed a significant decrease only at 8 weeks post-BDL (Fig. 3). As expected, the main brain osmolytes correlated more significantly with Gln than with NH_4^+ (Fig. 6).

Cr also continued to decrease until 8 weeks post-BDL ($-$11%). The continuous decrease in Cr (also tCr) during the disease may be due to the direct toxic effect of NH_4^+ through inhibition of the enzyme arginine:glycine amidinotransferase involved in Cr synthesis,[72] to the release of Cr by astrocytes in response to osmotic stress,[40] or both. The overall and progressive decrease in Cr in CLD brain may in turn lead to cellular energy dysfunction, through decreased cellular capacity to store energy rather than through direct PCr decrease, in keeping with our previous work demonstrating that PCr levels were stable in the same animal model using *in vivo* ^{31}P-MRS.[38]

Chronic HE has been linked repeatedly to disturbances in neurotransmission systems, although the mechanisms are incompletely understood.[17,20] The cognitive and motor alterations in HE are believed to be the result of altered neurotransmission, mainly glutamatergic and GABA-ergic.[51] Several metabolites involved in neurotransmission were reliably quantified in our study. Glu concentration dropped at 6 weeks post-BDL, together with a trend toward declining concentrations of Asp and GABA. Glu correlated strongly with brain Gln, while the correlation with plasma NH_4^+ was lower (Fig. 6), all findings in keeping with our previous data.[38] The presumed reduction in Glu could simply be the result of NH_4^+ detoxification driven by increased Gln synthesis from Glu in astrocytes. In support of this hypothesis, no significant changes in the Glu-Gln cycle between astrocytes and neurons were measured in a recent *in vivo* ^{13}C-MRS study performed in the same animal model.[73] The decline in Glu concentration may in turn induce the decrease in Asp, since the 2 metabolites are linked by transamination. Although not measurable by ^{1}H-MRS, this finding also raises the question of whether this change influences alpha-ketoglutarate. Based on present data, it is important to emphasize that these changes are likely to arise at terminal stages of disease.

Cerebral energy metabolism is believed to be altered in chronic HE, but findings on energy metabolism disturbances in chronic HE are inconsistent, and their direct role in the development and progression of brain oedema is not firmly established.[74] NH_4^+ acts as a neurotoxin interfering with cerebral metabolism and possibly with energy pathways. The secondary increase in Gln may impact energy metabolism through one of

several mechanisms: initial osmotic stress, changes in the Glu-Gln cycle, or deleterious effects of cytotoxic brain oedema. Lac, Cr and PCr, metabolites involved in energy metabolism, were reliably measured in our study (in particular separate detection of Cr from PCr). While Cr showed a decrease in the brain of BDL rats, Lac and PCr did not change significantly, in keeping with previous studies,[38,39] both in BDL rats. However, they contrast with a previous report performed on post mortem rats 6 weeks post-BDL[37] where increased cerebral Lac rather than Gln was suggested to be a key factor in the pathogenesis of brain oedema together with alterations in osmoregulation.

The presence of oxidative stress as measured by decreasing Asc levels continued to be noticeable at late stages of the study. GSH also showed a trend toward declining concentrations at 8 weeks post-BDL. GSH is present at lower concentrations than Asc in brain, and therefore its estimation showed some variations which hindered statistical analysis. Our previous study in a different brain region[38] showed no changes in brain Asc, while GSH tended to decrease by 8 weeks post-BDL. These different findings could reflect the differential vulnerability of distinct anatomical regions to CLD, something which requires further study.

Conclusions

Using a multimodal, *in vivo* and longitudinal approach we have shown that biologically relevant neurometabolic changes in a rat model of chronic HE are already noticeable 2 weeks after BDL, and progress throughout the 8 week course of the disease. The well-described increase in brain Gln in response to plasma NH_4^+ rise was confirmed, together with a decrease in brain Cr and Asc, both novel findings. Brain Gln and plasma NH_4^+ were closely correlated, and plasma NH_4^+ correlated significantly with the decrease in distance moved by the animals. In addition, Gln showed stronger correlations with other metabolites than plasma NH_4^+, suggesting that some of the changes are directly related to Gln increase rather than indirectly via NH_4^+ toxicity. A decrease in brain organic osmolytes mirrored the rise in brain Gln concentration. In addition, changes in astrocyte morphology together with an increase in AQP4 expression were observed as early as 4 weeks post-BDL, offering evidence that osmoregulation was incomplete in spite of these adaptive changes. To conclude, these early changes are suggestive of osmotic and oxidative stress and are the likely premise of any of several later factors known to be involved in HE pathogenesis. In addition, the novel finding of decreased cerebral Cr and Asc creates new opportunities to explore neuroprotective strategies for the treatment of HE.

Financial support

Financial support was provided by the SNSF project no 310030_173222/1, the EU: FP7-PEOPLE-2012-ITN project 316679 TRANSACT and by the CIBM (UNIL, UNIGE, HUG, CHUV, EPFL, as well as the Leenaards and Jeantet Foundations), the CHUV and the HUG.

Conflict of interest

The authors declare no conflicts of interest that pertain to this work.

Please refer to the accompanying ICMJE disclosure forms for further details.

Authors' contributions

OB: conceived the study, performed sample collection, acquired, analysed and interpreted data, and wrote/revised the manuscript. VR: performed sample collection, acquired, analysed and interpreted data and revised the manuscript. KP: performed sample collection, performed histological measures, analysed and interpreted histological data. JG: designed and analysed the data of the behavioural studies. VMcL: conceived and designed the study, analysed, interpreted data, wrote/revised the manuscript. CC: conceived and designed the study, performed BDL surgery and sample collection, acquired, analyzed, and interpreted data, and wrote/revised the manuscript.

Acknowledgements

The authors thank Dr Corina Berset (CIBM), Stefanita Mitrea (CIBM) for their help during BDL surgery, animal follow-up, sample collection and Marc Loup (CHUV), Dario Sessa (HUG) for their assistance with histology. The behavioural tests were performed in collaboration with the Laboratory of Behavioral Genetics of Prof. Carmen Sandi (EPFL).

Supplementary data

Supplementary data to this article can be found online at https://doi.org/10.1016/j.jhep.2019.05.022.

References

Author names in bold designate shared co-first authorship

[1] Blei AT, Ferenci P, Lockwood A, Mullen K, Tarter R, Weissenborn K. Hepatic encephalopathy – definition, nomenclature, diagnosis, and quantification: final report of the working party at the 11th World Congresses of Gastroenterology, Vienna, 1998. Hepatology 2002;35:716–721. https://doi.org/10.1053/jhep.2002.31250.
[2] Dharel N, Bajaj JS. Definition and nomenclature of hepatic encephalopathy. J Clin Exp Hepatol 2015;5:S37–S41. https://doi.org/10.1016/j.jceh.2014.10.001.
[3] Monfort P, Cauli O, Montoliu C, Rodrigo R, Llansola M, Piedrafita B, et al. Mechanisms of cognitive alterations in hyperammonemia and hepatic encephalopathy: therapeutical implications. Neurochem Int 2009;55:106–112. https://doi.org/10.1016/j.neuint.2009.01.021.
[4] Häussinger D, Sies H. Editorial: hepatic encephalopathy: clinical aspects and pathogenetic concept. Arch Biochem Biophys 2013;536:97–100. https://doi.org/10.1016/j.abb.2013.04.013.
[5] Chavarria L, Cordoba J. Magnetic resonance imaging and spectroscopy in hepatic encephalopathy. J Clin Exp Hepatol 2015;5:S69–S74. https://doi.org/10.1016/j.jceh.2013.10.001.
[6] Braissant O, McLin VA, Cudalbu C. Ammonia toxicity to the brain. J Inherit Metab Dis 2013;36:595–612. https://doi.org/10.1007/s10545-012-9546-2.
[7] Dasarathy S, Mookerjee RP, Rackayova V, Rangroo Thrane V, Vairappan B, Ott P, et al. Ammonia toxicity: from head to toe? Metab Brain Dis 2017;32:529–538. https://doi.org/10.1007/s11011-016-9938-3.
[8] Felipo V, Butterworth RF. Neurobiology of ammonia. Prog Neurobiol 2002;67:259–279, doi:S0301008202000199 [pii].
[9] Cooper AJ, Plum F. Biochemistry and physiology of brain ammonia. Physiol Rev 1987;67:440–519.
[10] Rama Rao KV, Norenberg MD. Glutamine in the pathogenesis of hepatic encephalopathy: the Trojan horse hypothesis revisited. Neurochem Res 2014;39:593–598. https://doi.org/10.1007/s11064-012-0955-2.
[11] Shawcross DL, Olde Damink SWM, Butterworth RF, Jalan R. Ammonia and hepatic encephalopathy: the more things change, the more they

remain the same. Metab Brain Dis 2005;20:169–179. https://doi.org/10.1007/s11011-005-7205-0.
[12] Norenberg MD. Distribution of glutamine synthetase in the rat central nervous system. J Histochem Cytochem 1979;27:756–762.
[13] Bémeur C, Cudalbu C, Dam G, Thrane AS, Cooper AJL, Rose CF. Brain edema: a valid endpoint for measuring hepatic encephalopathy? Metab Brain Dis 2016;31:1249–1258. https://doi.org/10.1007/s11011-016-9843-9.
[14] Brusilow SW, Koehler RC, Traystman RJ, Cooper AJL. Astrocyte glutamine synthetase in hyperammonemic syndromes potential target for therapy. Neurotherapeutics 2010;7:452–470. https://doi.org/10.1016/j.nurt.2010.05.015.
[15] Haussinger D, Kircheis G, Fischer R, Schliess F, vom Dahl S. Hepatic encephalopathy in chronic liver disease: a clinical manifestation of astrocyte swelling and low-grade cerebral edema? J Hepatol 2000;32:1035–1038, doi:S0168827800801105 [pii].
[16] Häussinger D. Low grade cerebral edema and the pathogenesis of hepatic encephalopathy in cirrhosis. Hepatology 2006;43:1187–1190. https://doi.org/10.1002/hep.21235.
[17] Ott P, Vilstrup H. Cerebral effects of ammonia in liver disease: current hypotheses. Metab Brain Dis 2014;29:901–911. https://doi.org/10.1007/s11011-014-9494-7.
[18] Rama Rao KV, Jayakumar AR, Norenberg MD. Induction of the mitochondrial permeability transition in cultured astrocytes by glutamine. Neurochem Int 2003;43:517–523. https://doi.org/10.1016/S0197-0186(03)00042-1.
[19] Hadjihambi A, Arias N, Sheikh M, Jalan R. Hepatic encephalopathy: a critical current review. Hepatol Int 2017;12:135–147. https://doi.org/10.1007/s12072-017-9812-3.
[20] Cagnon L, Braissant O. Hyperammonemia-induced toxicity for the developing central nervous system. Brain Res Rev 2007;56:183–197. https://doi.org/10.1016/j.brainresrev.2007.06.026.
[21] Rodrigo R, Cauli O, Gomez-Pinedo U, Agusti A, Hernandez-Rabaza V, Garcia-Verdugo JM, et al. Hyperammonemia induces neuroinflammation that contributes to cognitive impairment in rats with hepatic encephalopathy. Gastroenterology 2010;139:675–684. https://doi.org/10.1053/j.gastro.2010.03.040.
[22] Azhari H, Swain MG. Role of peripheral inflammation in hepatic encephalopathy. J Clin Exp Hepatol 2018;8:281–285. https://doi.org/10.1016/j.jceh.2018.06.008.
[23] Butterworth RF. The liver-brain axis in liver failure: neuroinflammation and encephalopathy. Nat Rev Gastroenterol Hepatol 2013;10:522–528. https://doi.org/10.1038/nrgastro.2013.99.
[24] Coltart I, Tranah TH, Shawcross DL. Inflammation and hepatic encephalopathy. Arch Biochem Biophys 2013;536:189–196. https://doi.org/10.1016/j.abb.2013.03.016.
[25] Shah NJ, Neeb H, Kircheis G, Engels P, Häussinger D, Zilles K. Quantitative cerebral water content mapping in hepatic encephalopathy. Neuroimage 2008;41:706–717. https://doi.org/10.1016/j.neuroimage.2008.02.057.
[26] Jover R, Rodrigo R, Felipo V, Insausti R, Saez-Valero J, Garcia-Ayllon MS, et al. Brain edema and inflammatory activation in bile duct ligated rats with diet-induced hyperammonemia: a model of hepatic encephalopathy in cirrhosis. Hepatology 2006;43:1257–1266. https://doi.org/10.1002/hep.21180.
[27] Kale RA, Gupta RK, Saraswat VA, Hasan KM, Trivedi R, Mishra AM, et al. Demonstration of interstitial cerebral edema with diffusion tensor MR imaging in type C hepatic encephalopathy. Hepatology 2006;43:698–706. https://doi.org/10.1002/hep.21114.
[28] McPhail MJW, Taylor-Robinson SD. The role of magnetic resonance imaging and spectroscopy in hepatic encephalopathy. Metab Brain Dis 2010;25:65–72. https://doi.org/10.1007/s11011-010-9171-4.
[29] Córdoba J, Sanpedro F, Alonso J, Rovira A. 1H magnetic resonance in the study of hepatic encephalopathy in humans. Metab Brain Dis 2002;17:415–429. https://doi.org/10.1023/A:1021926405944.
[30] Kreis R, Farrow N, Ross BD. Localized 1H NMR spectroscopy in patients with chronic hepatic encephalopathy. Analysis of changes in cerebral glutamine, choline and inositols. NMR Biomed 1991;4:109–116.
[31] Rudler M, Weiss N, Perlbarg V, Mallet M, Tripon S, Valabregue R, et al. Combined diffusion tensor imaging and magnetic resonance spectroscopy to predict neurological outcome before transjugular intrahepatic portosystemic shunt. Aliment Pharmacol Ther 2018;48:863–874. https://doi.org/10.1111/apt.14938.
[32] Lanz B, Rackayova V, Braissant O, Cudalbu C. MRS studies of neuroenergetics and glutamate/glutamine exchange in rats: extensions to hyperammonemic models. Anal Biochem 2017;529:245–269. https://doi.org/10.1016/j.ab.2016.11.021.
[33] Cudalbu C. In vivo studies of brain metabolism in animal models of hepatic encephalopathy using 1H magnetic resonance spectroscopy. Metab Brain Dis 2013;28:167–174. https://doi.org/10.1007/s11011-012-9368-9.
[34] Mlynárik V, Cudalbu C, Xin L, Gruetter R. NMR spectroscopy of rat brain in vivo at 14.1 Tesla: improvements in quantification of the neurochemical profile. J Magn Reson 2008;194:163–168. https://doi.org/10.1016/j.jmr.2008.06.019.
[35] Tkáč I, Öz G, Adriany G, Uğurbil K, Gruetter R. In vivo 1H NMR spectroscopy of the human brain at high magnetic fields: metabolite quantification at 4T vs. 7T. Magn Reson Med 2009;62:868–879. https://doi.org/10.1002/mrm.22086.
[36] Butterworth RF, Norenberg MD, Felipo V, Ferenci P, Albrecht J, Blei AT, et al. Experimental models of hepatic encephalopathy: ISHEN guidelines. Liver Int 2009;29:783–788. https://doi.org/10.1111/j.1478-3231.2009.02034.x.
[37] Bosoi CR, Zwingmann C, Marin H, Parent-Robitaille C, Huynh J, Tremblay M, et al. Increased brain lactate is central to the development of brain edema in rats with chronic liver disease. J Hepatol 2014;60:554–560. https://doi.org/10.1016/j.jhep.2013.10.011.
[38] Rackayova V, Braissant O, McLin VA, Berset C, Lanz B, Cudalbu C. 1H and 31P magnetic resonance spectroscopy in a rat model of chronic hepatic encephalopathy: in vivo longitudinal measurements of brain energy metabolism. Metab Brain Dis 2016;31:1303–1314. https://doi.org/10.1007/s11011-015-9715-8.
[39] Chavarria L, Oria M, Romero-Giménez J, Alonso J, Lope-Piedrafita S, Cordoba J, et al. Brain magnetic resonance in experimental acute-on-chronic liver failure. Liver Int 2013;33:294–300. https://doi.org/10.1111/liv.12032.
[40] Bothwell JH, Rae C, Dixon RM, Styles P, Bhakoo KK. Hypo-osmotic swelling-activated release of organic osmolytes in brain slices: Implications for brain oedema in vivo. J Neurochem 2001;77:1632–1640. https://doi.org/10.1046/j.1471-4159.2001.00403.x.
[41] Strange K. Cellular volume homeostasis. AJP Adv Physiol Educ 2004;28:155–159. https://doi.org/10.1152/advan.00034.2004.
[42] Rackayova V, Cudalbu C, Pouwels PJW, Braissant O. Creatine in the central nervous system: from magnetic resonance spectroscopy to creatine deficiencies. Anal Biochem 2017;529:144–157. https://doi.org/10.1016/j.ab.2016.11.007.
[43] Rae CD. A guide to the metabolic pathways and function of metabolites observed in human brain 1H magnetic resonance spectra. Neurochem Res 2014;39:1–36. https://doi.org/10.1007/s11064-013-1199-5.
[44] Ong JP, Aggarwal A, Krieger D, Easley KA, Karafa MT, Van Lente F, et al. Correlation between ammonia levels and the severity of hepatic encephalopathy. Am J Med 2003;114:188–193. https://doi.org/10.1016/S0002-9343(02)01477-8.
[45] Laubenberger J, Haussinger D, Bayer S, Gufler H, Hennig J, Langer M. Proton magnetic resonance spectroscopy of the brain in symptomatic and asymptomatic patients with liver cirrhosis. Gastroenterology 1997;112:1610–1616. https://doi.org/10.1016/S0016-5085(97)70043-X.
[46] Singhal A, Nagarajan R, Hinkin CH, Kumar R, Sayre J, Elderkin-Thompson V, et al. Two-dimensional MR spectroscopy of minimal hepatic encephalopathy and neuropsychological correlates in vivo. J Magn Reson Imaging 2010;32:35–43. https://doi.org/10.1002/jmri.22216.
[47] Bajaj JS, Wade JB, Sanyal AJ. Spectrum of neurocognitive impairment in cirrhosis: Implications for the assessment of hepatic encephalopathy. Hepatology 2009;50:2014–2021. https://doi.org/10.1002/hep.23216.
[48] Leke R, Oliveira DL, Forgiarini LF, Escobar TD, Hammes TO, Meyer FS, et al. Impairment of short term memory in rats with hepatic encephalopathy due to bile duct ligation. Metab Brain Dis 2013;28:187–192. https://doi.org/10.1007/s11011-012-9347-1.
[49] Leke R, de Oliveira DL, Mussulini BHM, Pereira MS, Kazlauckas V, Mazzini G, et al. Impairment of the organization of locomotor and exploratory behaviors in bile duct-ligated rats. PLoS One 2012;7. https://doi.org/10.1371/journal.pone.0036322.
[50] **Hadjihambi A, Harrison IF, Costas-Rodríguez M, Vanhaecke F, Arias N, Gallego-Durán R, et al. Impaired brain glymphatic flow in experimental hepatic encephalopathy. J Hepatol 2018;70:40–49. https://doi.org/10.1016/j.jhep.2018.08.021.**
[51] Felipo V. Hepatic encephalopathy: effects of liver failure on brain function. Nat Rev Neurosci 2013;14:851–858. https://doi.org/10.1038/nrn3587.
[52] Görg B, Schliess F, Häussinger D. Osmotic and oxidative/nitrosative stress in ammonia toxicity and hepatic encephalopathy. Arch Biochem Biophys 2013;536:158–163. https://doi.org/10.1016/j.abb.2013.03.010.

[53] Bosoi CR, Rose CF. Oxidative stress: a systemic factor implicated in the pathogenesis of hepatic encephalopathy. Metab Brain Dis 2013;28:175–178. https://doi.org/10.1007/s11011-012-9351-5.
[54] Rice ME, Russo-Menna I. Differential compartmentalization of brain ascorbate and glutathione between neurons and glia. Neuroscience 1997;82:1213–1223. https://doi.org/10.1016/S0306-4522(97)00347-3.
[55] Bosoi CR, Yang X, Huynh J, Parent-Robitaille C, Jiang W, Tremblay M, et al. Systemic oxidative stress is implicated in the pathogenesis of brain edema in rats with chronic liver failure. Free Radic Biol Med 2012;52:1228–1235. https://doi.org/10.1016/j.freeradbiomed.2012.01.006.
[56] **Davies NA, Wright G, Ytrebø LM, Stadlbauer V, Fuskevåg OM, Zwingmann C, et al. L-ornithine and phenylacetate synergistically produce sustained reduction in ammonia and brain water in cirrhotic rats. Hepatology 2009;50:155–164. https://doi.org/10.1002/hep.22897.**
[57] **Wright G, Vairappan B, Stadlbauer V, Mookerjee RP, Davies NA, Jalan R. Reduction in hyperammonaemia by ornithine phenylacetate prevents lipopolysaccharide-induced brain edema and coma in cirrhotic rats. Liver Int 2012;32:410–419. https://doi.org/10.1111/j.1478-3231.2011.02698.x.**
[58] Cudalbu C, Taylor-Robinson SD. Brain edema in chronic hepatic encephalopathy. J Clin Exp Hepatol 2019. https://doi.org/10.1016/j.jceh.2019.02.003.
[59] Keep RF, Hua Y, Xi G. Brain water content: a misunderstood measurement? Transl Stroke Res 2012;3:263–265. https://doi.org/10.1007/s12975-012-0152-2.
[60] Bothwell JH, Styles P, Bhakoo KK. Swelling-activated taurine and creatine effluxes from rat cortical astrocytes are pharmacologically distinct. J Membr Biol 2002;185:157–164. https://doi.org/10.1007/s00232-001-0121-2.
[61] Hanna-El-Daher L, Braissant O. Creatine synthesis and exchanges between brain cells: what can be learned from human creatine deficiencies and various experimental models? Amino Acids 2016;48:1877–1895. https://doi.org/10.1007/s00726-016-2189-0.
[62] Braissant O, Henry H, Loup M, Eilers B, Bachmann C. Endogenous synthesis and transport of creatine in the rat brain: an in situ hybridization study. Mol Brain Res 2001;86:193–201. https://doi.org/10.1016/S0169-328X(00)00269-2.
[63] Wallimann T, Wyss M, Brdiczka D, Nicolay K, Eppenberger HM. Intracellular compartmentation, structure and function of creatine kinase isoenzymes in tissues with high and fluctuating energy demands: the ''phosphocreatine circuit'' for cellular energy homeostasis. Biochem J 1992;281:21–40. https://doi.org/10.1042/bj2810021.
[64] Rama Rao KV, Norenberg MD. Aquaporin-4 in hepatic encephalopathy. Metab Brain Dis 2007;22:265–275. https://doi.org/10.1007/s11011-007-9063-4.
[65] Wright G, Soper R, Brooks HF, Stadlbauer V, Vairappan B, Davies NA, et al. Role of aquaporin-4 in the development of brain oedema in liver failure. J Hepatol 2010;53:91–97. https://doi.org/10.1016/j.jhep.2010.02.020.
[66] Hernández-Rabaza V, Cabrera-Pastor A, Taoro-González L, Malaguarnera M, Agustí A, Llansola M, et al. Hyperammonemia induces glial activation, neuroinflammation and alters neurotransmitter receptors in hippocampus, impairing spatial learning: reversal by sulforaphane. J Neuroinflamm 2016;13:1–11. https://doi.org/10.1186/s12974-016-0505-y.
[67] Weiss N, Jalan R, Thabut D. Understanding hepatic encephalopathy. Intensive Care Med 2017;44:231–234. https://doi.org/10.1007/s00134-017-4845-6.
[68] Hiba O El, Elgot A, Ahboucha S, Gamrani H. Differential regional responsiveness of astroglia in mild hepatic encephalopathy: an Immunohistochemical approach in bile duct ligated rat. Acta Histochem 2016;118:338–346. https://doi.org/10.1016/j.acthis.2016.03.003.
[69] Wright G, Sharifi Y, Newman T, Davies N, Vairappan B, Perry H, et al. Characterisation of temporal microglia and astrocyte immune responses in bile duct-ligated rat models of cirrhosis. Liver Int 2014;34:1184–1191. https://doi.org/10.4016/3530.01.
[70] Brand A, Richter-Landsberg C, Leibfritz D. Multinuclear NMR studies on the energy metabolism of glial and neuronal cells. Dev Neurosci 1993;15:289–298. https://doi.org/10.1159/000111347.
[71] Lei H, Berthet C, Hirt L, Gruetter R. Evolution of the neurochemical profile after transient focal cerebral ischemia in the mouse brain. J Cereb Blood Flow Metab 2009;29:811–819. https://doi.org/10.1038/jcbfm.2009.8.
[72] Braissant O, Cagnon L, Monnet-Tschudi F, Speer O, Wallimann T, Honegger P, et al. Ammonium alters creatine transport and synthesis in a 3D culture of developing brain cells, resulting in secondary cerebral creatine deficiency. Eur J Neurosci 2008;27:1673–1685. https://doi.org/10.1111/j.1460-9568.2008.06126.x.
[73] **Baker L, Lanz B, Andreola F, Ampuero J, Wijeyesekera A, Holmes E, et al. New technologies – new insights into the pathogenesis of hepatic encephalopathy. Metab Brain Dis 2016;31:1259–1267. https://doi.org/10.1007/s11011-016-9906-y.**
[74] Rama Rao KV, Norenberg MD. Brain energy metabolism and mitochondrial dysfunction in acute and chronic hepatic encephalopathy. Neurochem Int 2012;60:697–706. https://doi.org/10.1016/j.neuint.2011.09.007.